Neutron Diffraction Study of the Magnetic Long-Range Order in Tb

O. W. DIETRICH AND J. ALS-NIELSEN
Danish Atomic Energy Commission, Research Establishment Risö, Roskilde, Denmark

(Received 31 March 1967)

Like other heavy rare-earth metals, Tb exhibits a magnetic phase with a spiral structure. This appears within the temperature region from 216 to 226°K between the ferromagnetic phase and the paramagnetic phase. The transition between ferromagnetic and spiral structure is of first order and implies no change in the long-range order. In the close vicinity of the Néel temperature $T_N=226$°K the spiral magnetic long-range order varies as $(T_N-T)^{0.25\pm0.01}$, whereas the total order within a wider temperature range roughly follows $(T_N-T)^{1/3}$. The turn angle per layer varies from 16.5° at 216°K to 20.7° at 226°K. The temperature variation of the transverse magnetostriction has also been measured and was found to vary approximately in proportion to the square of the magnetic long-range order.

1. INTRODUCTION

THE study of magnetism in the rare-earth metals has revealed the existence of phases with complex periodic magnetic order. The stability of such structures can be qualitatively explained[1] by a long-range indirect exchange interaction of the oscillating Ruderman-Kittel type between the localized magnetic moments, transmitted through the conduction electrons. A general survey of the magnetic structures at various temperatures for the rare earths has been given by Koehler[2] based on neutron diffraction measurements.

We have carried out a more detailed study of Tb. The main purpose of this experiment was the measurement of the critical magnetic scattering above the Néel temperature, the results of which are reported elsewhere.[3] This paper deals essentially with the temperature dependence of the magnetic moment.

Tb forms a hexagonal closed-packed lattice. At low temperatures the spins are ferromagnetically aligned in the hexagonal planes, but at 216°K there is a first-order transition to a spiral structure, in which the spins still lie in the hexagonal planes, but turned through an angle from plane to plane, as sketched in Fig. 1. The turn angle in Tb is around 20°, varying a few degrees with temperature. At 226°K there is a transition of second order to the paramagnetic phase.

The magnetic order is reflected in the neutron diffraction pattern. Neutron scattering from the ferromagnetically aligned spins peaks at the reciprocal lattice points and is superposed on the nuclear scattering peaks. The spiral spin arrangement gives rise to satellite peaks displaced from the reciprocal lattice points in the direction of the hexagonal axis.

The diffraction pattern from the spiral structure may be understood in the following way; the spin at a lattice point with lattice vector $\mathbf{r}_i$ may be written as

$$\mathbf{S}_i=s_i\mathbf{S}_{i,\mathrm{sp}}+s_{i\perp}\mathbf{S}_{i\perp} \qquad (1)$$

where $\mathbf{S}_{i,\mathrm{sp}}$ is the vector $\{\cos(\mathbf{q}\cdot\mathbf{r}_i), \sin(\mathbf{q}\cdot\mathbf{r}_i), 0\}$ and $\mathbf{S}_{i\perp}$ is a vector perpendicular to $\mathbf{S}_{i,\mathrm{sp}}$. In the spiral phase $\mathbf{q}$ is finite, so that the thermodynamic average $\langle s_\perp\rangle=0$ and at the same time $\langle s\rangle\neq0$. The long-range-order scattering cross section is

$$\frac{d\sigma}{d\Omega}\propto\exp[-2W(\boldsymbol{\kappa})]\,|f(\boldsymbol{\kappa})|^2\sum_{ij}\exp[i\boldsymbol{\kappa}\cdot(\mathbf{r}_i-\mathbf{r}_j)]\times\sum_{\alpha\beta}\left(\delta_{\alpha\beta}-\frac{\kappa_\alpha\kappa_\beta}{\kappa^2}\right)\langle S_i^\alpha\rangle\langle S_j^\beta\rangle. \qquad (2)$$

Here $\boldsymbol{\kappa}=\mathbf{k}_0-\mathbf{k}$ is the scattering vector, i.e., the difference between the incoming and outgoing neutron wave vectors, $f(\boldsymbol{\kappa})$ is the form factor, $\exp[-2W(\boldsymbol{\kappa})]$ is the Debye-Waller factor, and α and β symbolize the Cartesian coordinates x, y and z.

Inserting the spiral spin representation (1) in (2), we find

$$\frac{d\sigma}{d\Omega}\propto\tfrac{1}{4}\langle s\rangle^2\sum_\tau\delta(\boldsymbol{\kappa}-(\boldsymbol{\tau}\pm\mathbf{q}))\,|f(\boldsymbol{\kappa})|^2\left(1+\frac{\kappa_z^2}{\kappa^2}\right)\times\exp[-2W(\boldsymbol{\kappa})], \qquad (3)$$

which indicates that diffraction occurs for $\boldsymbol{\kappa}=\boldsymbol{\tau}\pm\mathbf{q}$, with an intensity proportional to $\langle s\rangle^2$, that is, to the square of the magnetic long-range order.

The peak positions and the peak intensities have been measured accurately for $\boldsymbol{\kappa}$ around the (0, 0, 2) or (0, 0, 4) reciprocal lattice points and their satellites as a function of temperature within the regions of the magnetic transitions.

The experimental setup is described briefly in Sec. 2, and the temperature dependence of the magnetic long-range order as derived from the central and satellite peak intensities is given in Sec. 3. The turn angle per layer, $\frac{1}{2}qc$, where c is the hexagonal lattice constant, is discussed in Sec. 4, and finally in Sec. 5 the results are given of a remeasurement of the hexagonal lattice constant $c(T)$, as determined from the position of the ferromagnetic and nuclear (0, 0, 4) peak. Because of magnetostriction, the change in magnetic structure is connected with an anomalous variation of the lattice constant with temperature.

[1] R. J. Elliott, Phys. Rev. **124**, 346 (1961).
[2] W. C. Koehler, J. Appl. Phys. **36**, 1078 (1965).
[3] J. Als-Nielsen and O. W. Dietrich (to be published).

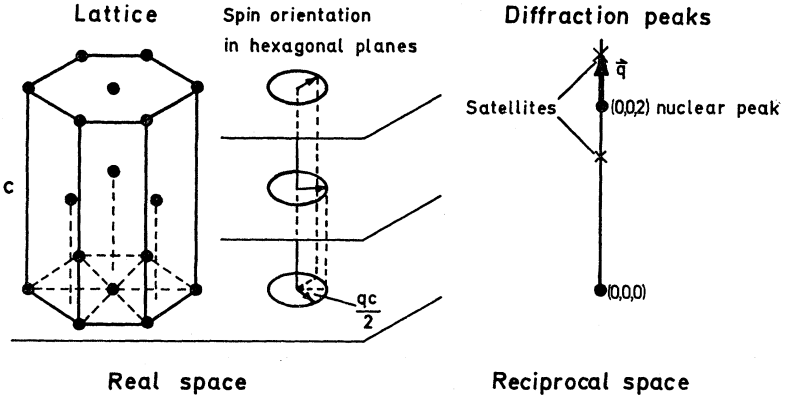

FIG. 1. The spiral magnetic structure in Tb (hcp) with the spins aligned in the basal planes, but turned an angle $\frac{1}{2}(qc)$ from plane to plane. This structure gives rise to satellites in the neutron-diffraction pattern displaced a distance q from the reciprocal lattice points in the direction of the hexagonal axis.

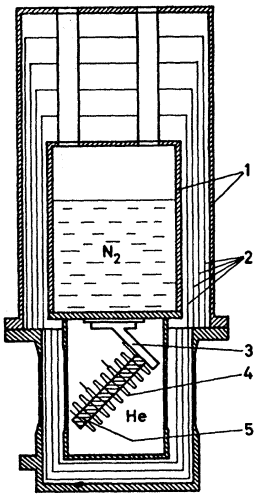

FIG. 2. The nitrogen cryostat. 1. Al housing, 2. Thermal shields (Mo foils), 3. Perspex rod, 4. Heating-coil system, 5. Tb crystal in Al container.

2. APPARATUS

The neutron diffractometer has previously been described.[4] In this experiment the neutron wavelengths were 1.56 Å or 2.15 Å. The Tb single crystal[5] was a rod of approximately 6 mm diam and 50 mm length. It was mounted in the liquid-nitrogen cryostat shown in Fig. 2. The crystal was encapsuled in an aluminum container screwed on a Perspex rod which was mounted on the bottom of the liquid-nitrogen bath. The sample housing was filled with He gas to ensure temperature homogeneity. The aluminum container was surrounded by a heating-coil system consisting of three separate coils in series, allowing adjustment for thermal gradients along the rod. Temperatures were measured at the middle and at the ends of the rod by means of copper-constantan thermocouples welded to the surface of the aluminum container. The thermocouples were calibrated

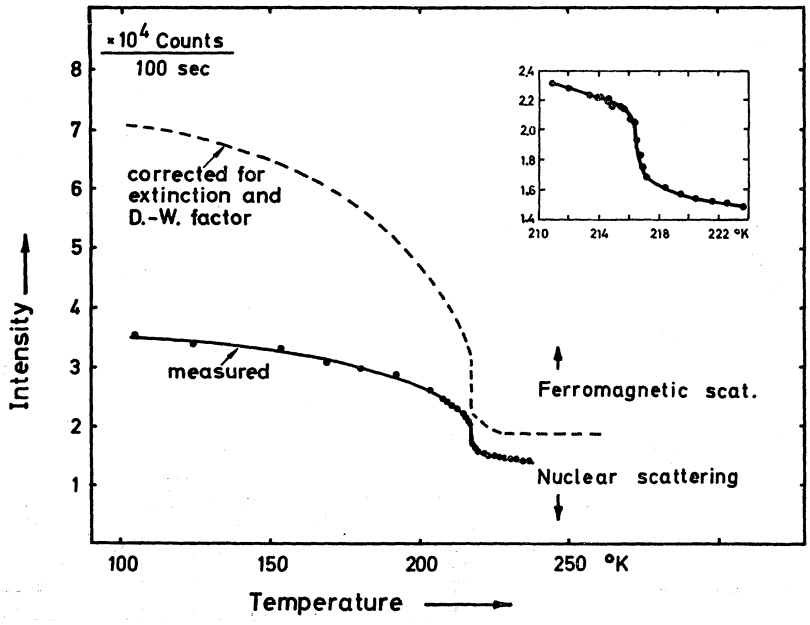

FIG. 3. Temperature variation of the ferromagnetic and nuclear scattering peak intensity at the (0, 0, 4) reciprocal lattice point. The dashed curve is the data corrected for extinction and Debye-Waller factor. The corrected nuclear part of the scattering intensity above the transitions is independent of temperature and can be subtracted to obtain the ferromagnetic scattering intensity.

[4] J. Als-Nielsen and O. W. Dietrich, Phys. Rev. 153, 706, 711, 717 (1967).
[5] The crystal was grown from the melt by Metals Research, Cambridge, England.

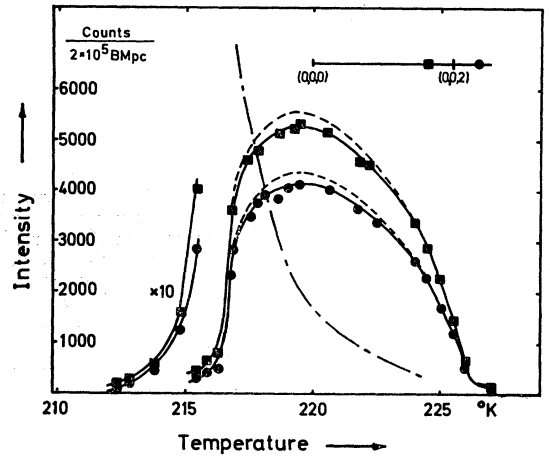

FIG. 4. Temperature variation of the (0, 0, 2) satellite peak intensities. The difference in intensity for the two satellites is due to the form factor and to geometrical effects. The dashed curves are corrected for extinction. The ferromagnetic part of the (0, 0, 2) peak intensity is also shown. A small amount of ferromagnetic order remains in the spiral region probably due to strains and inhomogeneities in the crystal. (BMpc at the intensity scale reads Beam Monitor preset counts.)

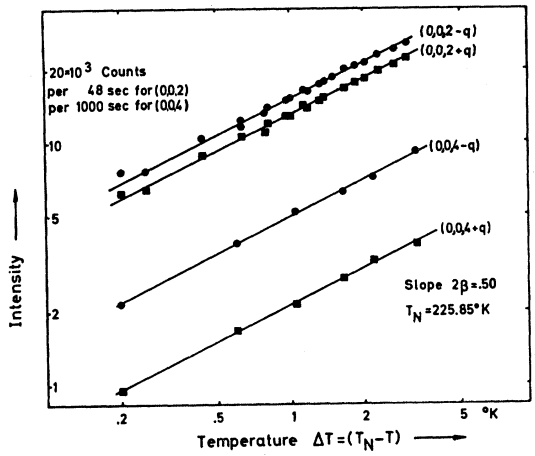

FIG. 6. Double-logarithmic plot of the corrected spiral peak intensities close to T_N versus $\Delta T = T_N - T$. The weighted peak intensities were least-square fitted to the power law $(T_N - T)^{2\beta}$ for different choices of T_N. The best fits were obtained for $T_N = 225.85°K$ and $2\beta = 0.50$ with estimated uncertainties of ± 0.05 and 0.02°K, respectively.

against a precision platinum resistance thermometer, giving confidence to the determination of the absolute value of the Néel temperature, for which some divergence is found in the literature. An electronic control system kept the temperature of the sample constant within $\pm 0.01°$.

3. TEMPERATURE DEPENDENCE OF MAGNETIC MOMENT

The determination of the ferromagnetic long-range order from measurements of the ferromagnetic scattering intensity is complicated by the superposition of the ferromagnetic scattering on the nuclear scattering peak, by the large extinction in the crystal, and by the inhomogeneities in the crystal.

The solid line in Fig. 3 shows the temperature variation of the (0, 0, 4) peak intensity, where the extinction is less than at (0, 0, 2), although still very important. The intensity remaining at high temperature is the nuclear scattering decreasing with temperature due to the Debye-Waller factor. The excess over the nuclear scattering is the ferromagnetic peak intensity. From the insertion in the figure, which is a magnification of the transition region from the ferromagnetic to the spiral structure, it is seen that the slope of the intensity curve changes abruptly near 216°K with a sharp decrease of the ferromagnetic intensity. This behavior is interpreted as due to a first-order transition near 216°K. The small tail above the transition temperature is probably due to strains or other types of inhomogeneities in the crystal. A ferromagnetic tail in the spiral

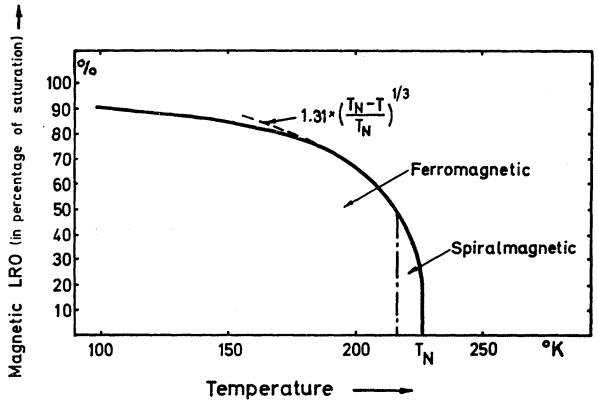

FIG. 5. Temperature variation of the total magnetic long-range order showing the smooth variation over the transition, indicated by the dashed-dotted line at 216°K. The dashed curve is the best fit of the theoretically predicted "⅓-law."

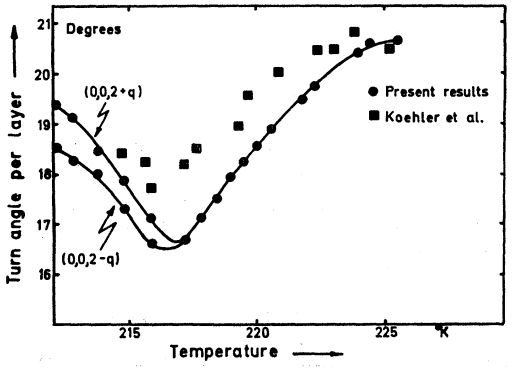

FIG. 7. Temperature variation of the spiral turn angle per layer as measured by the positions of the (0, 0, 2) satellites. Previous results by Koehler (Ref. 2) are shown for comparison.

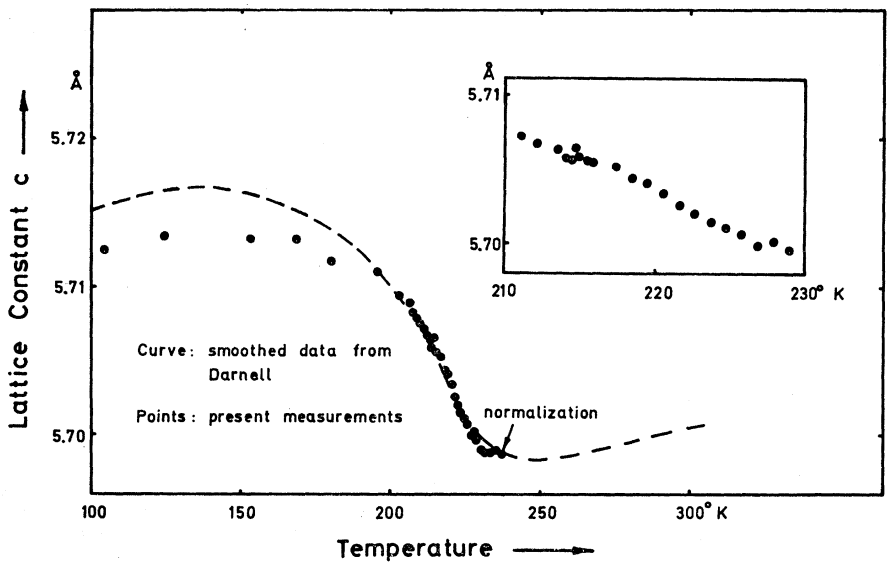

FIG. 8. Variation of the hexagonal lattice constant c with temperature as measured by the position of the nuclear and ferromagnetic (0, 0, 4) reflection. The data are normalized at 237°K to previous x-ray data by Darnell (Ref. 14). The insertion is a magnification over the transition regions.

region was also observed by Koehler *et al.*[6] and by Arrott *et al.*[7]

The extinction correction is large and will therefore be discussed in some detail. The Bragg scattered intensity I from a mosaic crystal with mosaic spread η can be calculated by means of a Monte Carlo technique, where the collimators, the wavelength distribution, and the sample shape are simulated on a computer. It is convenient to calculate I versus the variable $\Sigma=QD/\eta$, where D is a suitable linear dimension in the crystal and $Q=\lambda^3F^2N^2/\sin 2\theta$ in standard notation. For the magnetic scattering, F depends on temperature through $\langle s\rangle$. For small values of Σ, I will be proportional to Σ, but for larger values the curve $I(\Sigma)$ will level off and this is the extinction effect. The extinction correction can thus be inferred directly from $I(\Sigma)$, if the absolute value of Σ is known. A direct estimate of Σ is not very accurate, but the superposition of ferromagnetic and nuclear scattering allows an accurate determination of the scaling of the I versus Σ curve. Assuming 90% ferromagnetic saturation at 100°K,[8] the ratio between the nuclear and magnetic scattering intensities for an extinction-free crystal can be calculated. A comparison with the measured ratio determines thus the extinction at 100°K. From the $I(\Sigma)$ curve, we then found Σ at 100°K and the extinction for any measured intensity. This Σ-value at 100°K agrees with a direct estimate within 10%. The peak intensity corrected for extinction and Debye-Waller factor is shown as the dashed line in Fig. 3.

The smearing out of the ferromagnetic to spiral transition is also seen in the onset of spiral order as shown in Fig. 4. The points are the intensities of the (0, 0, 2) satellites, and the dashed curves are the intensities corrected for extinction. The spiral structure dominates above 217°K, but can be detected down to 212°K. The tail above the second-order transition at 226°K is the peak intensity of the critical scattering.

The total magnetic long-range order, calculated as the sum of the ferromagnetic and spiral long-range order, is given versus temperature in Fig. 5, normalized to 90% saturation at 100°K.[8] The long-range order varies smoothly over the transition at 216°K within an estimated experimental uncertainty of 10%. The dashed-dotted line indicates the separation of ferromagnetic and spiral long-range order expected for a perfect crystal.

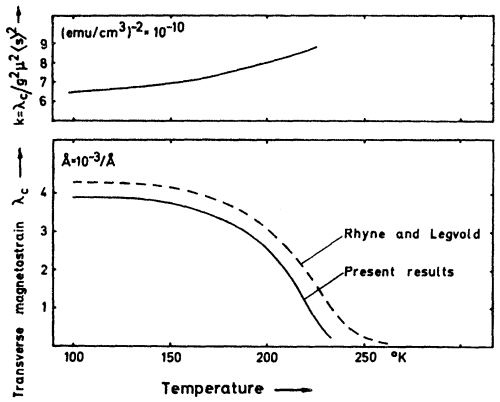

FIG. 9. Transverse magnetostrain versus temperature. Results of strain-gauge measurements by Rhyne and Legvold (Ref. 15) are also shown. The upper part shows the ratio between the magnetostrain and the square of the long-range order.

[6] W. C. Koehler, H. R. Child, E. O. Wollan, and J. W. Cable, J. Appl. Phys. **34**, 1335 (1963).
[7] A. Arrott, S. A. Werner, M. J. Cooper, R. Nathans, and G. Shirane, 12th Conference on Magnetism, Washington, D. C., 1966 (unpublished).
[8] D. E. Hegland, S. Legvold, and F. H. Spedding, Phys. Rev. **131**, 158 (1963).

According to the theory of lattice statistics[9] the long-range order is expected to decrease in the vicinity of the transition temperature as a power law

$$\text{LRO}=D_T[(T_N-T)/T_N]^\beta$$

with $\beta=\frac{1}{3}$ and $D_T\approx 1.5$. As shown in Fig. 5 the experimentally determined long-range order agrees with the "$\frac{1}{3}$ law" above 190°K for $D_T=1.31$. However, in the temperature region a few degrees below the Néel temperature a detailed analysis has shown that the spiral order varies as the power law $(T_N-T)^{1/4}$, as seen in the double-logarithmic plot Fig. 6, of the (0, 0, 2) and (0, 0, 4) satellite intensities versus $\Delta T=T_N-T$. The intensities were corrected for extinction, for a constant background count rate, and for the peak intensity of the critical scattering below T_N. The latter has been deduced from measurements[3] of the critical scattering above T_N, following the procedure outlined in Ref. 4. A weighted least-squares fit of the corrected satellite peak intensities to the power law $I=c(T_N-T)^{2\beta}$ was carried out, determining the best values of T_N and β. All four satellites gave consistent results with $T_N=225.85\pm 0.05$°K and $\beta=0.25\pm 0.01$. The best fits are shown in Fig. 6. The fact that the (0, 0, 2) and the (0, 0, 4) satellites, having different extinction, gave the same results gives confidence to the extinction correction and to the quoted β-value.

4. TEMPERATURE VARIATION OF THE SPIRAL TURN ANGLE

The positions of the satellite peaks in reciprocal space determined the turn angle of the spiral [Eq. (3)]. Figure 7 shows the measured turn angle from the satellites around the (0, 0, 2) reciprocal lattice point as a function of temperature. Measurements by Koehler[2] are also shown. In the region from about 217 to 226°K, the two satellites lie symmetrically around the central peak. Below 217°K this symmetry breaks down, the (0, 0, $2+q$) peak being farther displaced from the central peak than the (0, 0, $2-q$) peak. This effect is not understood in detail but, since the asymmetry in the satellites accompanies the onset of ferromagnetic ordering, it may be associated with the splitting of the energy bands of different spins which this induces.

The variation of q with temperature has been treated theoretically by several authors, using the free-electron theory. A change in the type or degree of magnetic order may change q through three mechanisms: the occurrence of magnetic superzones, the modification of the energy bands due to ferromagnetic ordering, and the change in the electronic mean free path due to magnetic disorder scattering, which modifies the Ruderman-Kittel interaction. Using the superzone theory, Elliott and Wedgwood[10] found that the spiral turn angle decreases in proportion to increasing spiral long-range order. This is in qualitative agreement with the measured turn angle variation in the spiral region, since the long-range order as seen by the conduction electrons is an average over regions comparable in size with the range of interaction. This microscopic order is believed to follow the ideal temperature dependence of Fig. 5, having maximum at 216°K, rather than the temperature dependence of the smeared macroscopic average over the whole crystal measured by the satellite intensities. The increase of q below 216°K is probably because of the onset of ferromagnetism.

The absolute values of the turn angles disagree with those predicted by the free-electron theory,[10–12] but this is to be expected, since the bands of the rare earths are known to be very different from those of the free-electron model.[13]

5. TRANSVERSE MAGNETOSTRICTION

The change in magnetic order is accompanied by a distortion of the crystal lattice due to magnetostriction. The variation of the hexagonal lattice constant c with temperature has been measured by determining the (0, 0, 4) peak position. The results are shown as filled circles in Fig. 8, using the x-ray data of Darnell[14] for normalization at 237°K. The agreement between the two sets of data is excellent in the transition region but some divergence is seen at lower temperatures. The insertion in the figure is a magnification within the transition region, showing no abrupt changes at the transition temperatures.

Rhyne and Legvold[15] have measured the c-axis strain in Tb by strain-gauge methods. In order to find the transverse magnetostrain, we have extrapolated the linear region of the thermal expansion around 300°K from Ref. 15 to lower temperatures, taking the temperature dependence of the thermal linear expansion coefficient into account through the Grüneisen expression.[15] The excess over the extrapolated expansion is ascribed to magnetostrain and is shown in Fig. 9. The present results lie somewhat below those of Rhyne and Legvold, which are also shown in the figure.

Generally, the magnetostrain can be expanded in terms of the magnetic long-range order. To the first nonvanishing order the transverse magnetostrain λ_c is proportional to the square of the long-range order,[16] $\lambda_c\approx kg^2\mu^2\langle s\rangle^2$, where k involves terms of the first-order magnetostriction tensor. In the upper part of Fig. 9, we have plotted the ratio k between λ_c and $g^2\mu^2\langle s\rangle^2$. The ratio k varies only slightly with temperature, indicating

[9] M. E. Fisher, J. Math. Phys. **4**, 278 (1963).
[10] R. J. Elliott and F. A. Wedgwood, Proc. Phys. Soc. (London) **84**, 63 (1964).
[11] P. G. deGennes and D. Saint-James, Solid State Commun. **1**, 62 (1963).
[12] H. Miwa, Proc. Phys. Soc. (London) **85**, 1197 (1965).
[13] J. O. Dimmock and A. J. Freeman, Phys. Rev. Letters **13**, 750 (1964).
[14] F. J. Darnell, Phys. Rev. **132**, 1098 (1963).
[15] J. J. Rhyne and S. Legvold, Phys. Rev. **138**, 507 (1965).
[16] W. P. Mason, Phys. Rev. **96**, 302 (1954).

a small negative fourth-order contribution in the expansion of λ_c.

6. CONCLUSION

The present neutron-diffraction study has yielded the following additional information about the magnetic structures of Tb.

(a) The magnetic long-range order follows the characteristic temperature variation of spontaneous magnetization with $T_N=226°K$. For temperatures above $0.9T_N$ there is good agreement with the power law $(T_N-T)^\beta$ with $\beta=\frac{1}{3}$ except in a region few degrees below T_N where $\beta=\frac{1}{4}$. The transition between the ferromagnetic and spiral phase is of first order and occurs at 216°K without any change of the long-range order.

(b) The spiral turn angle per layer has a minimum at the ferromagnetic to spiral transition temperature. This is in agreement with the superzone theory which predicts that the turn angle should decrease with increase of spiral long-range order. The quantitative agreement between theories based on the free-electron model and the experiment is poor, but this is not surprising since the rare earths are known to have electronic structures very different from the free-electron model.

(c) The ferromagnetic long-range order $\langle s \rangle$ has been correlated with the lattice expansion λ_c due to magnetostriction, and reasonable agreement with the approximate relation $\lambda_c=kg^2\mu^2\langle s \rangle^2$ was observed.

ACKNOWLEDGMENT

The authors wish to express their gratitude to Professor A. R. Mackintosh for valuable discussions and criticism.

PHYSICAL REVIEW VOLUME 162, NUMBER 2 10 OCTOBER 1967

Nuclear Spin-Lattice Relaxation in Hexagonal Transition Metals: Titanium†

ALBERT NARATH
Sandia Laboratory, Albuquerque, New Mexico
(Received 15 May 1967)

The nuclear magnetic resonance of ^{47}Ti and ^{49}Ti has been observed in hexagonal close-packed titanium metal in the temperature range $T=1$–$4°K$. Measurements of the line profile and relaxation rates were carried out at 12.5 MHz by pulsed nuclear resonance techniques. Since the gyromagnetic ratios of ^{47}Ti and ^{49}Ti are nearly identical, the resonances of the two isotopes were superimposed. A partially resolved first-order quadrupole spectrum having a total width exceeding 8 kOe was observed, yielding a probable assignment $h^{-1}e^2qQ^{47}\approx h^{-1}e^2qQ^{49}\approx 7.7$ MHz. The average Knight shift is estimated to be $K=(+0.4\pm0.2)\%$. The spin-lattice relaxation times T_1, which are quite long ($T_1T=150\pm20$ sec°K), provide evidence that the conduction-electron states at the Fermi level are predominantly *d*-like. The theory of nuclear spin-lattice relaxation in hexagonal transition metals is treated in the tight-binding approximation. Contact, core-polarization, orbital, and dipolar hyperfine interactions are considered. The magnitudes of the orbital and dipolar contributions to the spin-lattice relaxation rate depend on the orientation of the magnetic field relative to the hexagonal *c* axis. In the presence of *s-d* mixing, the contact contribution is found to interfere destructively with one of the components of the core-polarization contribution. The predicted total relaxation rates are shown to depend more strongly on the orbital admixture coefficients than is the case in cubic transition metals. The relatively large number of parameters in the theory precludes a unique fit to the experimental results for titanium. In general, however, the calculated rates exceed the observed rate by a factor of 2–3 over a wide range of parameter values. The apparent discrepancy is attributed to the combined effects of (1) the electron-phonon enhancement of the electronic specific heat and (2) *s-d* interference effects. The former effect causes the "bare" electron density of states to be overestimated, while the latter leads to an overestimate of the sum of contact and core-polarization contributions to the relaxation.

I. INTRODUCTION

DURING recent years considerable progress has been achieved in the utilization of conduction-electron-induced nuclear spin-lattice relaxation phenomena in the study of electronic properties of transition metals. To date, most theoretical and experimental efforts in this field have been concerned with metals having cubic structures. The important contributions to the observed relaxation rates have been shown to arise from core-polarization[1] and orbital[2] hyperfine interactions with the *d* component of the conduction-electron wave functions at the Fermi level, as well as from the familiar contact[3] hyperfine interaction with the *s* component. Conduction-electron contributions associated with magnetic-dipole[2] and electric-quadrupole[4,5] hyperfine interactions, on the other hand, are

† This work was supported by the U.S. Atomic Energy Commission.

[1] Y. Yafet and V. Jaccarino, Phys. Rev. **133**, A1630 (1964).
[2] Y. Obata, J. Phys. Soc. Japan **18**, 1020 (1963).
[3] J. Korringa, Physica **16**, 601 (1950).
[4] A. H. Mitchell, J. Chem. Phys. **26**, 1714 (1957).
[5] Y. Obata, J. Phys. Soc. Japan **19**, 2348 (1964).